Optical and Quantum Electronics (2019) 51:60
https://doi.org/10.1007/s11082-019-1776-1

On the reliability of pulse power saturation models for broad-area GaAs-based lasers

Joachim Piprek[1]

Received: 27 November 2018 / Accepted: 6 February 2019 / Published online: 14 February 2019

Abstract
With short current pulses, GaAs-based lasers can achieve high output powers if self-heating and catastrophic optical damage are suppressed. However, the pulse power is still severely limited by internal saturation mechanisms. Over the past decade, various power loss mechanisms have been identified by numerical laser simulation but published conclusions differ even for the same laser diode. We here investigate the reliability of such simulations and find that the error range remains relatively small if all saturation mechanisms are considered simultaneously in a self-consistent model, including a realistic hole mobility. Accurate pulse power predictions are demonstrated by simulating measurements on two different laser structures without making material parameter adjustments.

Keywords Laser diode · Pulse operation · Output power saturation · Numerical simulation

1 Introduction

High-power laser diodes are of great interest for various applications, from solid state laser pumping to automotive light detection and ranging (Tarasov 2010; Wenzel and Zeghuzi 2017; Knigge et al. 2018). In continuous-wave (CW) operation, the maximum power is usually limited by the self-heating of the laser (Piprek et al. 2002). Much higher laser power can be achieved with short current pulses if self-heating effects and catastrophic optical damage are suppressed (Wenzel et al. 2010b). Maximum pulse powers beyond 100 W have been reported for broad-area lasers based on GaAs (Tarasov et al. 2007). However, even with pulses as short as 10 ns, saturation effects severely limit the achievable power (Zeghuzi et al. 2018).

This article is part of the Topical Collection on Numerical Simulation of Optoelectronic Devices, NUSOD' 18.

Guest edited by Paolo Bardella, Weida Hu, Slawomir Sujecki, Stefan Schulz, Silvano Donati, Angela Traenhardt.

✉ Joachim Piprek
piprek@nusod.org

[1] NUSOD Institute LLC, Newark, DE 19714-7204, USA

Based on numerical Fabry–Perot laser models, several saturation mechanisms have been investigated in recent publications, including carrier leakage from the quantum wells (QWs), free-carrier absorption (FCA), two-photon absorption (2PA), gain compression, and longitudinal spatial hole burning (LSHB). As introduction to our reliability study, we briefly review these publications below.

Wang et al. (2010) employed a two-dimensional electro-optic model and identified electron leakage from the QWs as root cause of the power saturation. LSHB was also relevant. FCA was included in the model but the assumed FCA cross section was extremely small so that a large gain compression factor of $\varepsilon = 70 \times 10^{-17}$ cm^3 was needed to fit the measurement. This phenomenological parameter ε represents spectral hole burning, carrier heating, and similar non-equilibrium effects inside the quantum wells, which reduce the available optical gain at high photon densities. However, such fit parameter may also compensate for inaccuracies of the saturation model. Based on the same model, but using more realistic FCA cross-sections, Wenzel et al. (2010a) recognized the significant influence of FCA and carrier recombination inside the waveguide layers. Consequently, their fit parameter $\varepsilon = 0.8 \times 10^{-17}$ cm^3 is close to typical values (Wenzel and Zeghuzi 2017).

Using a one-dimensional traveling-wave optical model, Dogan et al. (2014) explained the power saturation solely by two-photon absorption (2PA) and subsequent free-carrier absorption. This secondary FCA effect is caused by 2PA-generated carriers and it was assumed proportional to the third power of the photon density, which is not correct since 2PA and FCA are separate processes (Piprek and Li 2018a). By using the carrier lifetime as fit parameter, the secondary FCA was identified as main saturation mechanism at high power. Carrier transport effects were ignored completely.

More recently, Avrutin and Ryvkin (2017) investigated the influence of carrier transport by solving the vertical carrier diffusion equation within the waveguide analytically, but without considering non-radiative carrier recombination. With the exception of strongly asymmetric waveguide designs, they concluded that both the primary and secondary 2PA effects are smaller than FCA caused by injected carriers, which the same authors previously identified as main saturation mechanism (Ryvkin and Avrutin 2006).

Most recently, Zeghuzi et al. (2018) employed a time-dependent multi-lateral-mode traveling-wave model. Carrier transport effects were included only in lateral direction, inside the active layer. Vertical carrier leakage from the active layer was ignored as well as free carrier accumulation in the waveguide. Gain compression was identified as main saturation mechanism with $\varepsilon = 18 \times 10^{-17}$ cm^3, followed by 2PA and LSHB. However, the authors concluded that lateral non-uniformities and time-dependent effects exert only minor influence on the saturation behavior of Fabry–Perot lasers.

All these studies investigated the pulse power saturation of very similar GaAs-based broad-area lasers with InGaAs quantum wells emitting light near 1 μm wavelength. Yet, the dominating saturation mechanisms were quite different. Such contradictions are often rooted in incomplete models which ignore some relevant mechanisms and instead use fit parameters to find agreement with measurements. Therefore, we recently developed a more comprehensive model that included all of the proposed saturation mechanisms self-consistently (Piprek and Li 2018a). In particular, 2PA and subsequent FCA were treated as separate processes after 2PA-generated carriers join the injected free carriers. Without any parameter fitting, the simulated pulse power was in close agreement with the measurement (Fig. 1). Figure 1 also plots results after step-wise removal of key mechanisms. LSHB shows some influence, but free-carrier absorption and electron leakage are clearly dominating, while 2PA and gain compression are negligible. This steady-state simulation ignored dynamic effects which were shown to act on a much shorter time-scale than our 300 ns

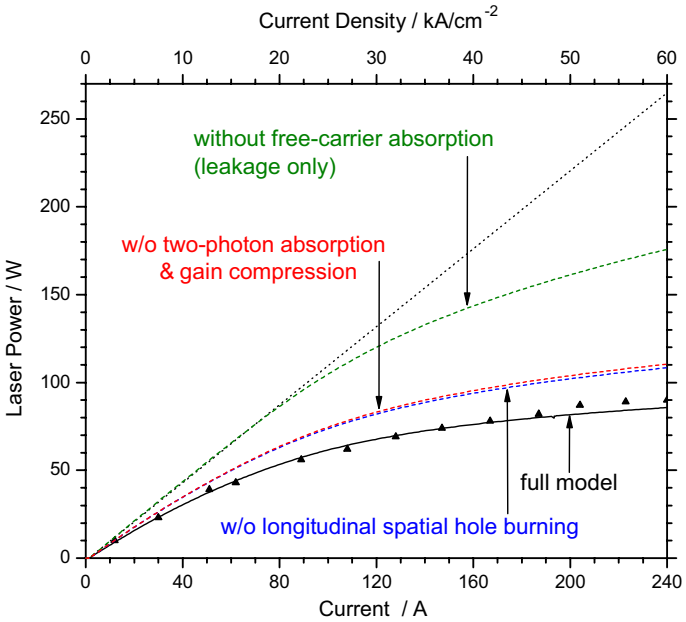

Fig. 1 Laser power versus current as measured (symbols) and as simulated (solid line). The dashed lines show the simulation results after subsequent removal of key saturation mechanisms from the model. The dotted line is a linear extension of the initial slope. Measured data are from Wenzel et al. (2010a), the simulations are explained in Piprek and Li (2018a)

current pulse (Zeghuzi et al. 2018). On the other hand, peak power measurements of short laser pulses are inherently difficult (Wang et al. 2010) but error bars were not provided for the measured data points (Wenzel et al. 2010a).

However, our simulations included a large number of material parameters, some of which are not exactly known. In the following, we investigate such uncertainties and the reliability of our model.

2 Models and parameters

Our analysis employs the laser simulation software PICS3D by Crosslight Software, which self-consistently combines carrier transport, quantum-well band structure, stimulated photon emission, and wave guiding. The transport model includes Fermi statistics, drift and diffusion of electrons and holes, their thermionic emission across hetero-interfaces, as well as carrier loss mechanisms such as Shockley–Read–Hall (SRH) recombination, spontaneous photon emission, and Auger recombination. The optical model considers photon scattering losses, free-carrier absorption (FCA), and two-photon absorption (2PA). 2PA-generated carriers and injected carriers follow the same transport mechanisms and both contribute to FCA. Gain compression is considered using the common parameter $\varepsilon = 10^{-17}$ cm^3 (Wenzel and Zeghuzi 2017). Since lateral variations have a negligible effect on the pulse power saturation of broad-are lasers (Wang et al. 2010; Zeghuzi et al. 2018), the

electro-optic equations are only solved in vertical and longitudinal direction. More model details are published elsewhere (Piprek 2003; Piprek and Li 2018a).

Our device example is the same laser that was previously simulated by different groups (Wenzel et al. 2010a, b; Dogan et al. 2014; Piprek and Li 2018a). The laser cavity length is L = 4 mm and the lasing stripe width is W = 0.1 mm with facet reflectivities of 0.01 at the front and 0.95 at the back. The laser structure includes an InGaAs/GaAs multi-quantum well (MQW) active region emitting at 1060 nm as well as an AlGaAs graded-index (GRIN) layer. Vertical profiles are plotted in Fig. 2 illustrating the electron leakage into the p-side waveguide layers where carriers pile up at the beginning of the GRIN layer due to the rising band gap. The MQW optical confinement factor $\Gamma = 0.021$ is in perfect agreement with previous studies. The guided laser mode is well confined within the GaAs waveguide layer, so that an uniform 2PA coefficient of $\beta = 26$ cm/GW can be employed as measured for GaAs at the same wavelength (Said et al. 1992). The FCA cross-section is 12×10^{-18} cm^2 for free holes and 4×10^{-18} cm^2 for free electrons, as used by most other authors (Wenzel et al. 2010a, b; Dogan et al. 2014; Piprek and Li 2018a). The threshold current of about 2A is governed by QW recombination losses. Inside the QWs, our model calculates the spontaneous recombination rate self-consistently from the emission spectrum, outside the common recombination coefficient $B = 10^{-10}$ cm^3/s is applied. The defect-related SRH lifetime τ_{SRH} is 2 ns inside and 100 ns outside the QWs. However, the Auger recombination coefficient C typically dominates the threshold current, it is 5×10^{-30} cm^6/s inside and 1.5×10^{-30} cm^6/s outside the QWs.

3 Sensitivity analysis

In the following, key material parameters are varied in order to study their impact on the simulated power saturation. A reasonable variation range is established by using parameter values from related publications. For comparison, the maximum power at 240 A is listed in Table 1 for each case separately (not cumulative). The final error range is plotted in Fig. 3.

Published results of FCA measurements are somewhat uncertain. The lower FCA cross-sections used by Avrutin and Ryvkin (2017) allow for more output power (line 2 in Table 1). No reliable FCA data are available for quantum wells and removal of FCA

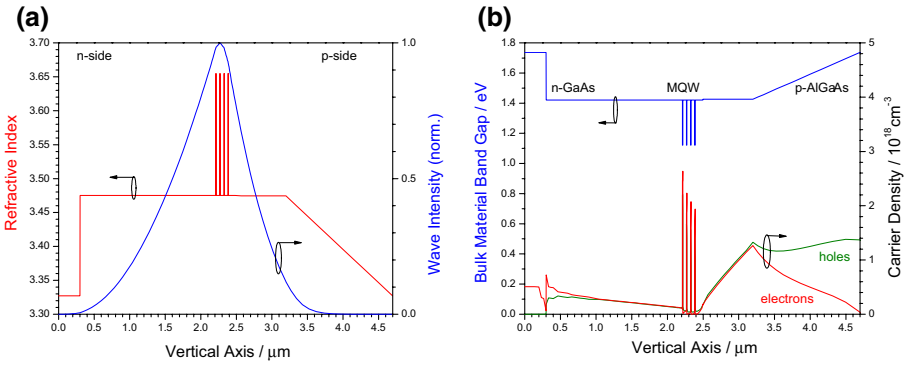

Fig. 2 Vertical profiles of **a** refractive index and wave intensity and **b** energy band gap and carrier density at the back facet at 240 A

Table 1 Comparison of simulated peak power values at 240A for different parameter variations in our model

	Model and parameter variation	Peak power (W)
1	Original	87
2	FCA cross section for electrons/holes = $3/10 \times 10^{-18}$ cm^2 (Avrutin and Ryvkin 2017)	95
3	No FCA in quantum wells (Piprek and Li 2018b)	90
4	QW: $\tau_{SRH} = 3$ ns, $B = 10^{-10} cm^3/s$, $C = 2\ 10^{-30} cm^6/s$ (Wenzel et al. 2010b)	87
5	$\tau_{SRH} = 3$ ns outside QW (Wenzel et al. 2010b)	82
6	Reduced gain as shown in Fig. 4 (Wenzel et al. 2010b)	84
7	10 degrees self-heating (Wang et al. 2010)	81
8	Band offset ratio = 65:35 (Piprek 2003)	87
9	Uniform hole mobility $\mu_p = 100$ cm^2/Vs	48
10	Uniform hole mobility $\mu_p = 200$ cm^2/Vs	85
11	Uniform hole mobility $\mu_p = 300$ cm^2/Vs	109
12	Uniform hole mobility $\mu_p = 400$ cm^2/Vs	124

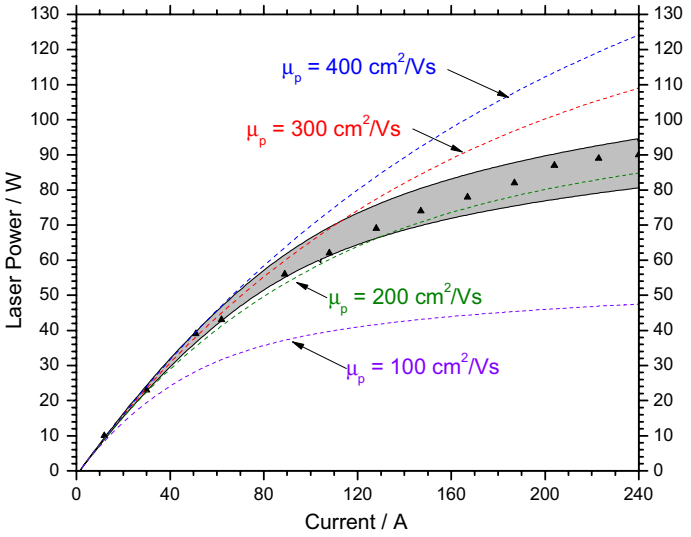

Fig. 3 Pulse power versus current error range and hole mobility variation (symbols: measurement)

from the quantum wells also reduces the power saturation (line 3). Two-photon absorption is insignificant in our case (Piprek and Li 2018a) and 2PA parameter variations have no effect.

Quantum well recombination losses control the threshold current but the Auger coefficient C is one of the most uncertain parameter in laser simulations (Piprek 2003). However, since our peak current is more than 100 times higher than the threshold current, QW recombination parameters have negligible influence here (line 4). But due to the strong carrier accumulation in the waveguide layers (Fig. 2b), reduction of the defect

recombination lifetime outside the QW from 100 ns to 3 ns leads to somewhat stronger saturation as it enhances the electron leakage from the MQW (line 5).

Leakage is also affected by the QW carrier density which depends on the QW gain. In fact, the gain model is at the hearth of any laser simulation. Wenzel et al. (2010b) employed a somewhat smaller gain in their model (Fig. 4) which leads to larger QW carrier density and slightly stronger saturation in our simulation (line 6). Gain compression effects are negligible in our case. But self-heating during pulsed laser operation reduces the gain. We here assume a temperature increase from 25 °C to 35 °C as estimated by Wang et al. (2010) for a very similar measurement, which reduces the output power to 81 W (line 7).

Another potentially critical parameter is the band offset at hetero-junctions. Thus far, we employed a band-offset ratio of 60:40 between conduction band and valence band. Increasing this ratio to 65:35 is expected to reduce electron leakage but it does not exert any significant influence on the output power in our case (line 8 in Table 1). Obviously, electron leakage is not controlled by the ability of electrons to escape from the QW, but rather by the ability of holes to get to the QWs (Wang et al. 2010). The hole mobility μ_p is much smaller than the electron mobility (Fig. 5) and it is this imbalance which enforces electron leakage into p-doped layers. In our original model, the mobility is influenced by alloy scattering and by doping and it is therefore non-uniform (Piprek 2003). Lines 9–12 in Table 1 show results with uniform hole mobility (dashed lines in Fig. 3). A uniform hole mobility of 200 cm^2/Vs produces almost the same saturation as the original model. However, a higher/lower hole mobility strongly reduces/increases the electron leakage from the MQW into the p-doped side, as shown in Fig. 6. Because the assumed hole mobility was not listed by other authors, it is not included in the error range shown as gray area in Fig. 3. The lower limit of this range is established by the self-heating effect (line 7) while the FCA reduction in line 2 gives the upper limit. Compared to the total power loss of 178 W at 240 A (Fig. 1), the error range amounts to ±4% and it fully contains the measured data.

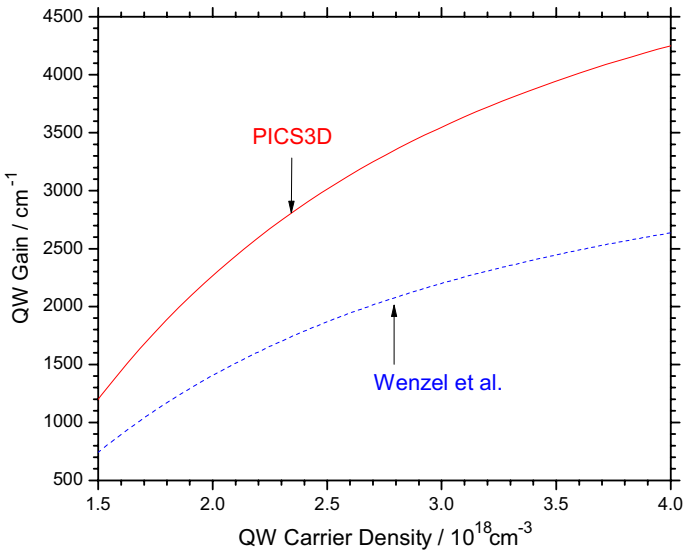

Fig. 4 Quantum well gain versus carrier density variation

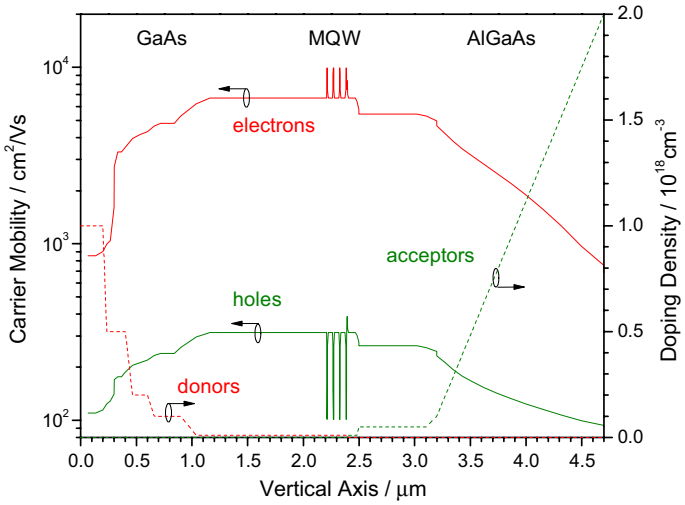

Fig. 5 Vertical profiles of carrier mobility and doping density

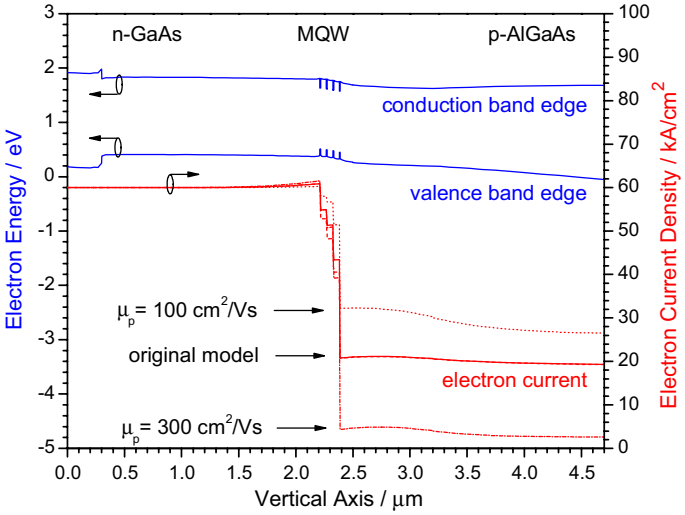

Fig. 6 Profiles of energy bands and 1D electron current density at 240 A for different hole mobilities

4 Reliability test

The reliability of our model can be further evaluated by its application to a different laser without changing any material parameters. We therefore simulate the structure given in (Veselov et al. 2014) featuring two InGaAs QWs embedded in an undoped 3 µm $Al_{0.1}Ga_{0.9}As$ waveguide layer that is sandwiched between n-doped $Al_{0.3}Ga_{0.7}As$ and p-doped $Al_{0.6}Ga_{0.4}As$. The laser cavity length is L = 2.6 mm and the lasing stripe width is W = 0.1 mm with cleaved facets on both sides (R = 0.3). Vertical profiles of energy band

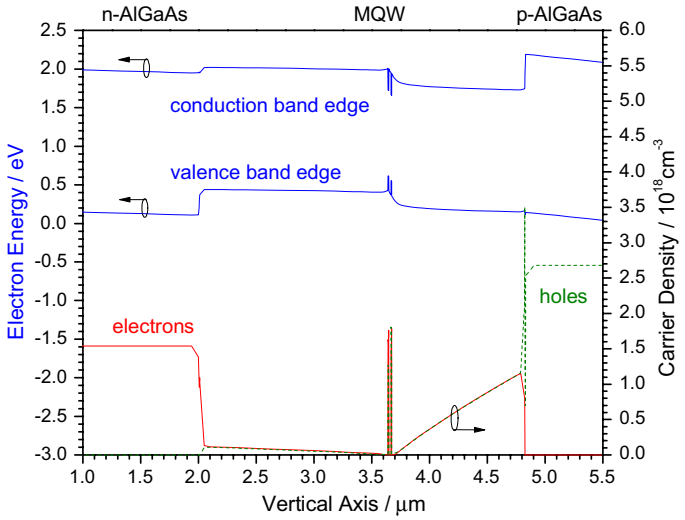

Fig. 7 Vertical energy band diagram and carrier den-sities at 30 kA/cm^2 current density

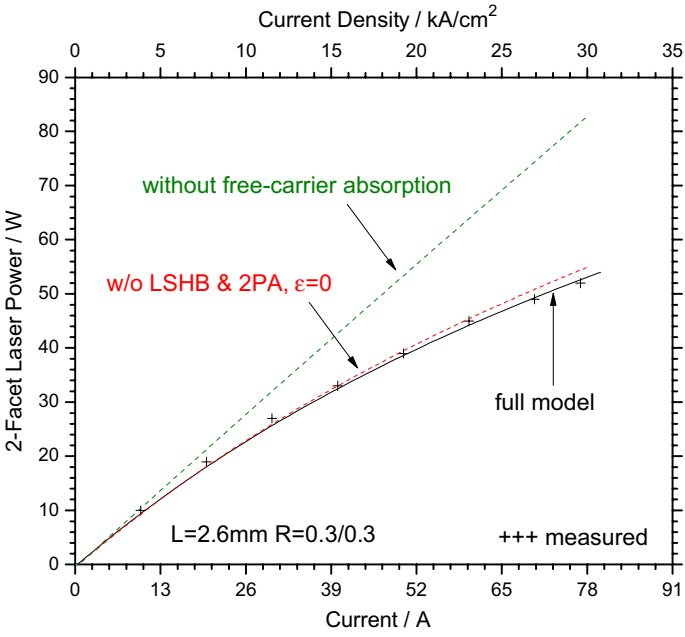

Fig. 8 Laser power versus current as measured (+++) and as simulated (lines). The dashed lines show results after subsequent removal of key saturation mechanisms from the model

edges and carrier concentrations are plotted in Fig. 7 at high injection. Figure 8 shows excellent agreement between our initial simulation and the reported measurement (Veselov et al. 2014). Subsequent removal of key mechanisms from the model produces the dashed

lines in Fig. 8. Longitudinal spatial hole burning (LSHB) has a negligible influence in such short symmetric cavities. Two-photon absorption (2PA) and gain compression (ε) are also irrelevant, as before. The final removal of free carrier absorption has the strongest effect and it produces an almost linear power versus current characteristic, even with double the current. Thus, hole mobility and electron leakage have much less influence on the pulse power saturation in this case, mainly due to the large conduction band barrier between waveguide and p-cladding (Fig. 7) which does not exist in the previous example. But carrier accumulation in the p-side waveguide layer (Fig. 7) enhances free-carrier absorption which dominates the power loss in this laser.

5 Summary

A reliable prediction of the pulse power saturation is demonstrated for two different broad-area InGaAs/GaAs Fabry–Perot lasers by self-consistent inclusion of all relevant saturation mechanisms in the simulation. Material parameter uncertainties produce a relatively small error range. However, hole mobility reductions by alloy scattering and doping must be accounted for as they control the electron leakage from the active layers.

References

Avrutin, E.A., Ryvkin, B.S.: Theory of direct and indirect effect of two-photon absorption on nonlinear optical losses in high power semiconductor lasers. Semicond. Sci. Technol. **32**, 015004 (2017)

Dogan, M., Michael, C.P., Zheng, Y., Zhu, L., Jacob, J.H.: Two photon absorption in high power broad area laser diodes. SPIE Proc. **8965**, 89650P (2014)

Knigge, A., Klehr, A., Wenzel, H., Zeghuzi, A., Fricke, J., Maaßdorf, A., Liero, A., Tränkle, G.: Wavelength-stabilized high-pulse-power laser diodes for automotive LiDAR. Phys. Status Solidi A **215**, 1700439 (2018)

Piprek, J., White, K., SpringThorpe, A.: What limits the maximum output power of long-wavelength AlGaInAs lasers? IEEE J. Quantum Electron. **38**, 1253–1259 (2002)

Piprek, J.: Semiconductor Optoelectronic Devices—Introduction to Physics and Simulation. Academic Press, San Diego (2003)

Piprek, J., Li, Z.M.: What causes the pulse power saturation of GaAs-based broad-area lasers? Photon. Technol. Lett. **30**, 963–966 (2018)

Piprek, J., Li, Z.M.: Evaluating two-photon absorption effects on pulsed high-power laser operation. In: 2018 NUSOD Conference Proceedings, IEEE, pp. 89–90 (2018b)

Ryvkin, B., Avrutin, E.: Non-uniform carrier accumulation in optical confinement layer as ultimate power limitation in ultra-high-power broad-waveguide pulsed InGaAs/GaAs/AlGaAs laser diodes. Electron. Lett. **42**, 1283–1284 (2006)

Said, A.A., Sheik-Bahae, M., Hagan, D.J., Wei, T.H., Wang, J., Young, J., Van Stryland, E.W.: Determination of bound-electronic and free-carrier nonlinearities in ZnSe, GaAs, CdTe, and ZnTe. J. Opt. Soc. Am. B **9**, 405–414 (1992)

Tarasov, I.S., Pikhtin, N.A., Slipchenko, S.O., Sokolova, Z.N., Vinokurov, D.A., Borschev, K.S., Kapitonov, V.A., Khomylev, M.A., Leshko, AYu., Lyutetskiy, A.V., Stankevich, A.L.: High power CW (16 W) and pulse (145 W) laser diodes based on quantum well heterostructures. Spectrochim. Acta Part A **66**, 819–823 (2007)

Tarasov, I.S.: High-power semiconductor separate-confinement double heterostructure lasers. Quantum Electron. **40**, 661–681 (2010)

Veselov, D.A., Kapitonov, V.A., Pikhtin, N.A., Lyutetskiy, A.V., Nikolaev, D.N., Slipchenko, S.O., Sokolova, Z.N., Shamakhov, V.V., Shashkin, I.S., Tarasov, I.S.: Saturation of light–current characteristics of high-power lasers (λ = 1.0–1.1 μm) in pulsed regime. Quantum Electron. **44**, 993–996 (2014)

Wang, X., Crump, P., Wenzel, H., Liero, A., Hoffmann, T., Pietrzak, A., Schultz, C.M., Klehr, A., Ginolas, A., Einfeldt, S., Bugge, F., Erbert, G., Tränkle, G.: Root-cause analysis of peak power saturation

in pulse-pumped 1100 nm broad area single emitter diode lasers. J. Quantum Electron. **46**, 658–665 (2010)

Wenzel, H., Crump, P., Pietrzak, A., Roder, C., Wang, X., Erbert, G.: The analysis of factors limiting the maximum output power of broad-area laser diodes. Opt. Quantum Electron. **41**, 645–652 (2010a)

Wenzel, H., Crump, P., Pietrzak, A., Wang, X., Erbert, G., Tränkle, G.: Theoretical and experimental investigations of the limits to the maximum output power of laser diodes. New J. Phys. **12**, 085007 (2010b)

Wenzel, H., Zeghuzi, A.: High-power lasers, Ch. 27. In: Piprek, J. (ed.) Handbook of optoelectronic device modeling and simulation. CRC Press, Boca Raton (2017)

Zeghuzi, A., Radziunas, M., Wünsche, H.-J., Klehr, A., Wenzel, H., Knigge, A.: Influence of nonlinear effects on the characteristics of pulsed high-power broad-area distributed Bragg reflector lasers. Opt. Quantum Electron. **50**, 88 (2018)